EIGHTEENTH EUROPEAN ROTORCRAFT FORUM

B - 17

Paper N° 74

# RECONSTRUCTION OF SPANWISE AIR LOAD DISTRIBUTION ON ROTORBLADES FROM STRUCTURAL FLIGHT TEST DATA

PROF. DR.-ING. DR. h.c.(H) H. ÖRY
DIPL.-ING. H. W. LINDERT
INSTITUT FÜR LEICHTBAU DER RWTH-AACHEN, GERMANY

September 15-18, 1992

AVIGNON, FRANCE

ASSOCIATION AERONAUTIQUE ET ASTRONAUTIQUE DE FRANCE

# RECONSTRUCTION OF SPANWISE AIR LOAD DISTRIBUTION ON ROTORBLADES FROM STRUCTURAL FLIGHT TEST DATA

Prof. Dr.-Ing. Dr.h.c.(H) H. Ö R Y
Dipl.-Ing. H.W. L I N D E R T

Institut für Leichtbau der RWTH-Aachen

Abstract

During flight tests, performed with Kamov-26 and Hughes 500E helicopters in Hungary, rotor blade structural response was measured with strain gauges applied to the blade. The measured response data were evaluated using a force reconstruction method developed at the Institut für Leichtbau at the University of Technology in Aachen, Germany. This method computes the acting air load forces on the rotating blade from measured blade response data.

For each helicopter a blade was prepared for testing and the structural parameters measured. Strain gauges were applied at specific spanwise locations. The flapping angle and azimuth position of the blade were recorded during flight testing. The signals from the blade instrumentation were transmitted by a telemetric system from the rotating rotor to a stationary receiving unit on the ground. Flight tests consisted of several hovering and forward flights at different flight speeds with both helicopters.

Reconstruction results of the spanwise air load forces are presented for both helicopter types. Reconstruction results for the Hughes helicopter at low flight speeds show Blade-Vortex-Interactions at the appropiate locations. This is also the case for some hovering flight test data evaluations.

Notation

| | | | |
|---|---|---|---|
| $[\ ]$ | vektor | $\{K\}$ | stiffnes matrix |
| $\{\ \}$ | matrix | $\{m\}$ | diagonal mass matrix |
| $\{\ \}^T$ | transposed matrix | $[\eta]_i$ | ith eigenvector |
| $[H]$ | generalized coordinate vektor | $\{\Phi\}$ | modal matrix |
| $[P]$ | force vektor | $\xi$ | damping |
| $[x]$ | blade deflection, deformation vektor | gen | generalized |
| $\{C\}$ | damping matrix | RM | reconstruction method |
| $\{E\}$ | elasticity matrix | BVI | blade-vortex-interactions |

Introduction

During flight helicopter rotor blades are submitted to periodically changing loads from aerodynamic and mass forces depending on the flight attitude. The blades and major parts of the rotor head assembly are subjected to extreme structural stressing. Furthermore strong interactions between the helicopter body and the rotor system occur from aerodynamic loads on the blades and from Blade-Vortex-Interactions (**BVI**). A satisfactory evaluation of such interactions and load distributions is only possible if the actual forces on the blade are exactly known in the time domain and their geometrical distribution. These forces can be obtained from computations with special computer codes, from measurements conducted in wind tunnels on model blades or as best from flight tests with full scale blades [Ref.1].

In this paper we would like to introduce an alternative method for obtaining the actual force distributions on rotating blades from windtunnel or flight test data. The proposed method allows the reconstruction of the blade forces in the time domain and their spanwise distribution from measured structural response data. These can be strain gauge, local accelarations or blade deformation data. With known blade structural parameters (e.g. elasticity matrix, eigenfrequencies, structural damping,

etc.) the forces and their distribution on the blade are computed using mechanical relations [Ref. 2,3,4]. From measured or computed blade deformations a computation of the selfinduced blade forces in a first approximation is possible [Ref.3].

In accordance with a co-operations agreement between the Technical University of Budapest, Hungary and the University of Technology in Aachen, Germany and with considerable help from the Hungarian Air Service, flight tests with helicopters were performed in the autumn of 1989, 1990 and 1991. The Hungarian Air Service permitted flight tests with Kamov-26 and Hughes 500E helicopters. A primary goal of the conducted flight tests was to verify the above mentioned RM with data from flight tests. Wind tunnel test data evaluation with the RM showed very good results [Ref.4].

Helicopters and Flight Testing

The russian build Kamov-26 Helicopter has a co-axial counterrotating rotor-system with two rotor planes 1,2m apart. The helicopter is powered by two nine cylinder radial engines located on both sides of the fuselage. It weighs about three metric tons and has a maximum flight speed of 160 km/h. Each rotor plane has three blades. The rotor radius is 6,5m. The blades are attached by a flapping hinge to the rotor shaft with practically no offset. The lag and pitch bearings are offset to the shaft by 0,6m. The blades are twisted by 11,5°, have a trapezoidal geometry and a NACA 230-12 profile. The blade spar is a rectangular, hollow, tapered beam composed of glas fiber reinforced composites (GFRP). The leading edge contains tubing and a lead counterweight. The trailing edge consists of foam material bonded to the spar. The outer blade skin is also made from GFRP and bonded to the upper and lower sides of the spar. Fig.1 shows the Kamov-26 before flight testing.

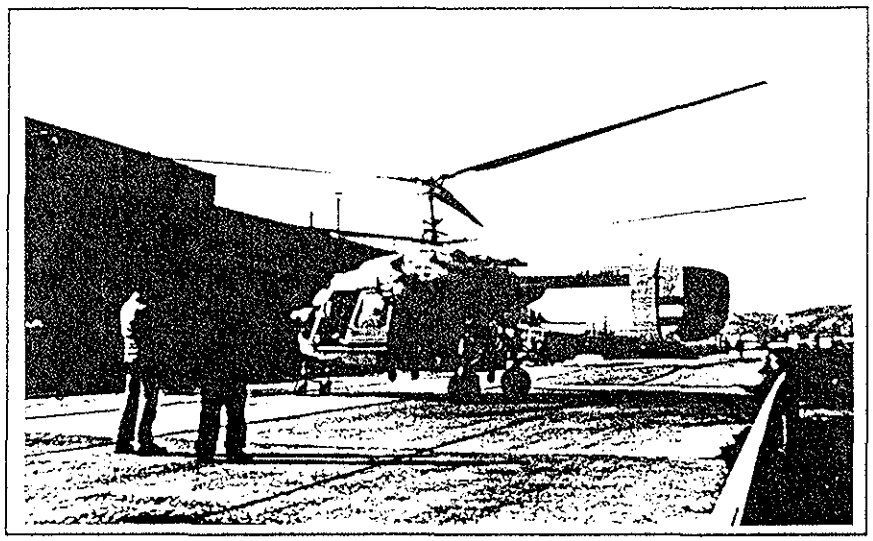

*Fig.1 Kamov-26 Helicopter*

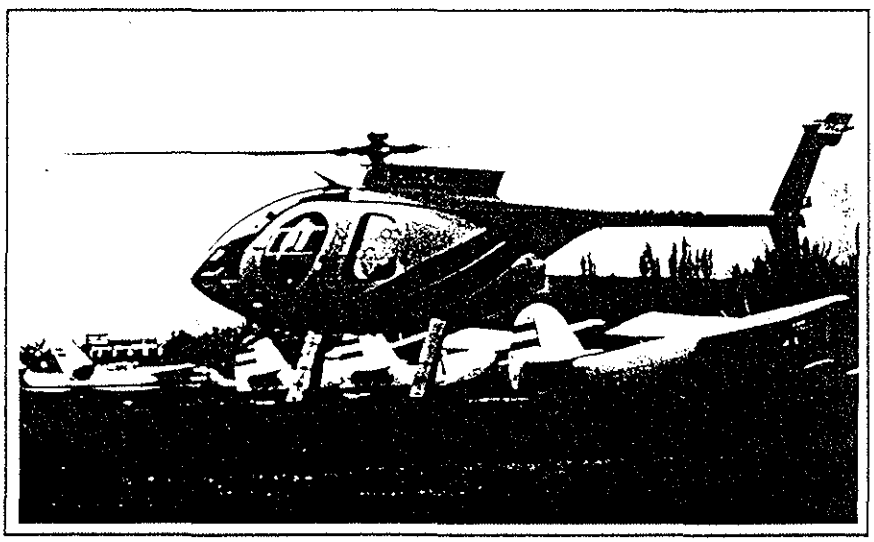

*Fig.2 Hughes 500E Helicopter*

The Hughes 500E helicopter has a five blade rotor and is powered by a turbine engine. It weighs 1-1,5 tons and has a maximum flight speed of 160-180 km/h. The rectangular blades have a NACA 0015 profile, a constant chord of 0,185m and are twisted by 8,5°. The blades are fixed to the rotor hub by aluminium/composite laminate "strap packs" which hold the centrifugal forces. The blade itself is attached to the hub by a combined flap-lag-pitch bearing. Fig.2 shows the Hughes helicopter in flight with the telemetric system mounted on the rotor hub.

At the airport of Budaörs near Budapest the test blades and the helicopters were prepared for flight testing. The flight test data was transmitted by a special telemetric system to a stationary receiving unit on the ground. During flight testing all signals (8 strain gauge, 1 flap angle, 1 azimuth position, 2 accelerometer signals) were recorded continuously on a data tape recorder. The helicopters flew along a prescribed test range and passed the receiving unit at close distance, constant flight speed and height. Flight speeds recorded for the Kamov-26 were 20, 40, 60, 80, 100, 120 and 140 km/h. Hughes test data was recorded for 20, 40, 60, 80 and 100 knots flight speed. Hovering test data was recorded for altitudes of 2, 10 and 20 meters.

Due to the low telemetric transmission power of 5 mWatts, test data from the helicopter at a greater distance of 150 meters to the receiving unit was of poor quality. In the test range the received test data quality was good to excellent. For each flight speed at least 15 rotor revolutions were recorded with excellent test data quality. Flight tests with the Kamov-26 were performed in autumn 1990 on three consecutive days yielding four test series of data. Hughes flight testing took place in autumn 1991 on four consecutive days and five test series were recorded. Each test serie consisted of several hovering flights at different altitudes and forward flights at the above mentioned flight speeds.

Reconstruction Method (Summary)

During rotation the blade experiences a constantly changing load resulting from aerodynamic and mass forces. These forces act on the blade structure and, due to the elastic properties of the blade, blade deformation results. The blade deformation thus describes the acting force distribution on the blade. This relation between the deformation and the acting forces is used in the RM to compute the air load distribution from the measured blade response data.

The RM has been presented in detail in Ref. 2,3,4. In this paper a brief summary of the principal theoretical background is given. In the following the blade is regarded as having motion and deformation in the flapping mode only since the recorded test data were obtained under this restriction. Coupling between flap, lag and pitch motion is neglected in a first approximation for the evaluation of the test data. In the RM a consideration of the coupling effects is possible [Ref. 3].

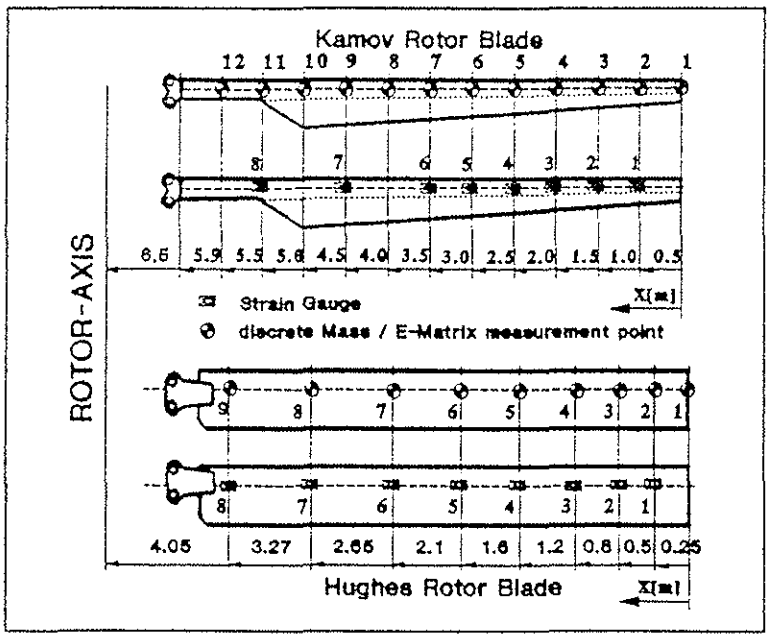


*Fig.3 discrete mass model of the blades and strain gauge locations*

The blade is modelled as a slender, linear elastic, hinged beam under centrifugal loading. Mass distribution is modelled in a lumped mass model representing the dynamic properties of the blade. Fig.3 shows the mass and strain gauge locations for the test blades. The elastic blade properties are given by the elasticity matrix (**E-matrix**) computed theoreticaly from known stiffness distribution or, as in our case, obtained from deformation measurements. The RM requires the modal parameters as well. These are e.g. the eigenmodes and frequencies of the rotating blade. Since measurement of the eigenmodes of the rotating blade is very difficult, they are computed from a numerically stiffened E-matrix taking in account the boundary conditions implied by the flap hinge [Ref.3,4].

The RM is based principally on the solution of the equation of motion for the modelled blade of Fig.3. In our case the inverse problem is solved. From measured blade response data the overall blade deformation is derived and from this the acting forces on the blade are computed.

A generalization of Eq.(1) yields a set of n uncoupled differential equations. The overall blade deflection [x] is approximated by a linear superposition of the natural blade eigenmodes as seen in Eq.(2). The matrix $\Phi$ is the modal matrix containing the eigenmodes of the rotating blade including the rigid body mode. The quantity H is the generalized coordinate of the SDOF systems defined by Eq.(5). Each singular equation in Eq.(5) represents the SDOF system for a natural eigenmode of the rotating blade written as in Eq.(6). This equation can be solved on the complex phase plane if certain conditions, e.g. proportional damping, are valid [Ref.3,4]. Fig.4 shows the complex phase plane for a SDOF system. The vectors R and the coordinate x represent the motion of the SDOF system.

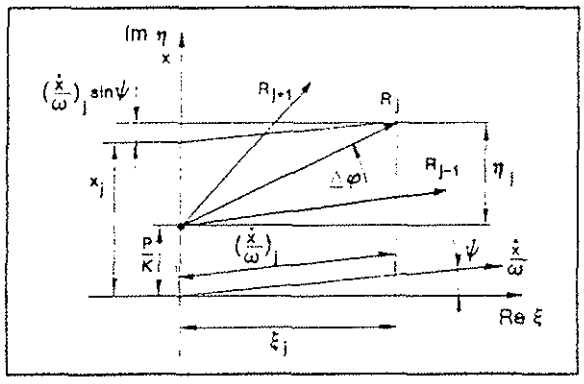


*Fig.4 invers phase plane geometric relations*

In Eq.(7) the geometric relations in Fig.4 required to solve Eq.(6) are stated. Certain conditions for the time history of P are required depending upon what blade deformation information is known [Ref. 4]. Is only the time history of the blade overall deflection x known, as it is in our case, Eq.(8) yields the sought generalized force P/K if x is substituted with the generalized coordinates H from Eq.(2) and with the restriction that the force P be constant during two time intervals dt (Fig.4). This assumption is valid if the time interval dt is small enough. The "graphic solution" of Eq.(6) on the phase plane with Eq.(7) and (8) is an invers problem and the method is thus called inverse phase plane method [Ref. 2,3,4].

(1) $$\{m\}[\ddot{x}] + \{C\}[\dot{x}] + \{K\}[x] = [P]$$

$$[x] = \sum_{i=1}^{n} [\eta]_i H_i = \{\Phi\}[H]$$

(2) $$[\dot{x}] = \sum_{i=1}^{n} [\eta]_i \dot{H}_i = \{\Phi\}[\dot{H}]$$

$$[\ddot{x}] = \sum_{i=1}^{n} [\eta]_i \ddot{H}_i = \{\Phi\}[\ddot{H}]$$

(3) $$\{\Phi\}^T\{m\}\{\Phi\}\,[\ddot{H}] + \{\Phi\}^T\{C\}\{\Phi\}\,[\dot{H}] + \{\Phi\}^T\{K\}\{\Phi\}\,[H] = \{\Phi\}^T\,[P_{(t)}]$$

(4)
$$\{\Phi\}^T\{m\}\{\Phi\} = \{m_{gen}\} \quad \textit{generalized mass}$$
$$\{\Phi\}^T\{C\}\{\Phi\} = \{C_{gen}\} \quad \textit{generalized damping}$$
$$\{\Phi\}^T\{K\}\{\Phi\} = \{K_{gen}\} \quad \textit{generalized stiffness}$$
$$\{\Phi\}^T[P] = [P_{gen}] \quad \textit{generalized force}$$

(5) $$\{\omega^2\}^{-1}[\ddot{H}] + \{K_{gen}\}^{-1}\{C_{gen}\}[\dot{H}] + [H] = \{K_{gen}\}^{-1}[P_{gen}]$$

(6) $$\frac{1}{\omega_j^2}\ddot{H}_j + \left(\frac{2\xi_{gen_j}}{\omega_j}\right)\dot{H}_j = \left(\frac{P_{gen}}{K_{gen}}\right)_j - H_j$$

(7) $$\sin\psi = \xi \quad \cos\psi = \sqrt{1-\xi^2} \quad \Delta t = t_j - t_{j-1}$$
$$\kappa = e^{-\xi\omega\Delta t} \quad \Delta\varphi = \omega\sqrt{1-\xi^2}\,\Delta t$$

(8) $$\frac{\kappa x_{j-1} - 2\cos(\Delta\varphi)\,x_j + \frac{1}{\kappa}x_{j+1}}{\kappa - 2\cos(\Delta\varphi) + \frac{1}{\kappa}} = \frac{P}{K}$$

(9) $$\sum_{i=1}^{k}\left(\left(\frac{\overline{P}_{gen}}{\overline{K}_{gen}}\right)_i - \overline{H}_i\right)\{m\}[\overline{\Phi}]_i\,\overline{\omega}_i^2 + \{K\}[x] = [P]$$

If all modal parameters of the blade are known a purely modal reconstruction is of course possible, but usually not all modal parameters are known. A modal reconstruction solving Eq.(5) then would lead to poor results depending on which modal parameters are used. In general not all modes are excited with equal intensity. If only a few or the significantly excited modes are known implementation of a method first suggested by Williams [Ref. 6] into the RM improves the solution considerably. This method is also called "mode acceleration method" by Craig [Ref.8]. Williams states that for an arbitrary force on a structure the response would be the quasistatic one resulting from elastic structural properties if the force were applied very slowly. On the other hand, if time history of the applied force were not quasistatic then the true dynamic forces resulting from mass inertia would have to be considered.

Integrating the idea of Williams into the reconstruction method leads to Eq.(9). The first left term describes the dynamic forces resulting from mass inertia and the blade motion. The second left term is the resulting elastic force if **[P]** were applied quasistatically to the blade. Eq.(9) results from substituting the first two left terms in Eq.(1) with the right terms of Eq.(6) (after appropiate matrix computations and transformations [Ref. 4]). If the generalized force **P/K** for each considered natural eigenmode of the rotating blade is then known from solving Eq.(6), Eq.(9) yields the sought force **[P]** on the blade.

As stated before the RM requires the significant modal parameters of the rotating blade. Due to the centrifugal influence the eigenmodes and frequencies will be different to those of the static blade since the blade structure experiences a stiffening in its elastic properties. In the case of a flap hinged blade a rigid body motion as first eigenmode results from centrifugal influence. Measurements of these eigenmodes during rotor rotation is very difficult if not impossible. The required eigenmodes and frequencies are therefor computed numerically and for this the E-matrix of the rotating blade must be known. Since a measurement of the stiffened E-Matrix is not easily performed the static E-matrix is stiffened numerically [Ref. 4] and from it the required eigenmodes and frequencies computed with a eigenvalue solving method.

The blade performs in-plane motions relative to the flap hinge resulting in selfinduced aerodynamic forces. These are contained in the reconstructed forces of Eq.(9). An evaluation of the selfinduced forces resulting from blade motion is possible, since the overall blade motion is known. A computation method is presented in Ref.3.

Preparation of the blades and helicopters

In preparation for flight testing the blade geometries and structural properties were measured. E-matrix measurements for the flapping mode were conducted at the mass locations shown in Fig.3. From the measured E-matrix eigenfrequencies were computed and compared with measured eigenfrequencies. A very good fit for the first four modes was achieved. This meant that the measured E-matrix was of good quality. After smoothing and optimization of the measured E-matrix a further comparison between measured and computed eigenfrequencies showed an excellent fit for the first six eigenmodes of the Kamov-26 and Hughes 500E blades. The E-matrix measurements showed linear elastic blade deformations in the required range for flight testing. The following table shows the eigenfrequencies for the blades.

| helicopter mode | Hughes 500E static | Hughes 500E 490 RPM | Kamov-26 static | Kamov-26 275 RPM |
|---|---|---|---|---|
| 1st mode | 1.46 Hz | 8.4 Hz | 0.96 Hz | 4.6 Hz |
| 2nd mode | 10.25 Hz | 22.2 Hz | 4.6 Hz | 11,7 Hz |
| 3rd mode | 28.80 Hz | 41.3 Hz | 11.8 Hz | 19,3 Hz |
| 4th mode | 57.20 Hz | 68.3 Hz | 21,3 Hz | 30.1 Hz |

Strain gauges were applied to the upper and lower sides of the blades at the locations depicted in Fig.3. These locations were chosen to optimize the measurement of the dynamic blade deformations. Gauge spacing was less in the outer blade region to account for expected aerodynamic effects and to achieve a higher resolution in this area. Since the blade structures were not to be damaged or altered, the gauges were applied directly to the blade surface. The wiring consisted of insulated copper wire of 0.25mm diameter. The wiring was bonded to the lower surface of the blade to ensure the least possible aerodynamic interference. Strain gauges and wiring were covered with very thin selfadhesive tape. During flight no negative experiences resulted from this application technique. Calibration of the gauges took place during the E-matrix measurements. The strain gauge signals from the flight tests define the elastic deformation of the blade. Transformation of these signals with the calibration factors yielded equivalent static bending moments. If these equivalent bending moments were applied to the static blade, the same blade deformation would result as experienced during flight testing. Combining the equivalent bending moments with the static E-matrix of the blade resulted in the elastic blade deformation required in the reconstruction method.

The flight test data was transmitted by a special telemetric system. This system can transmit twelve gauge or sensor signals simultaneously on a 240 MHz carrier frequency using a frequency multiplexing method. A stationary receiving unit on the ground processed the incoming signals and these were then transferred to a data tape recording system. The telemetric system consists of several small cylindrical modules placed in special holders and mounted to the helicopter rotor hubs. Fig.5 and Fig.6 show the mounted telemetric system. In Fig.5 the lower rotor hub assembly of the Kamov-26 is shown. The telemetric system is attached to the lag bearing of the test blade located in the lower part of Fig.5. Fig.6 shows the system in its aluminium holder mounted on top of the Hughes rotor hub. The steel strip extending forward from the lower part of the holder to the test blade root is the instrumentation for the flap angle measurement. The wiring of the strain gauges was soldered to a connection plate on the blades and from there connected to the telemetric system.

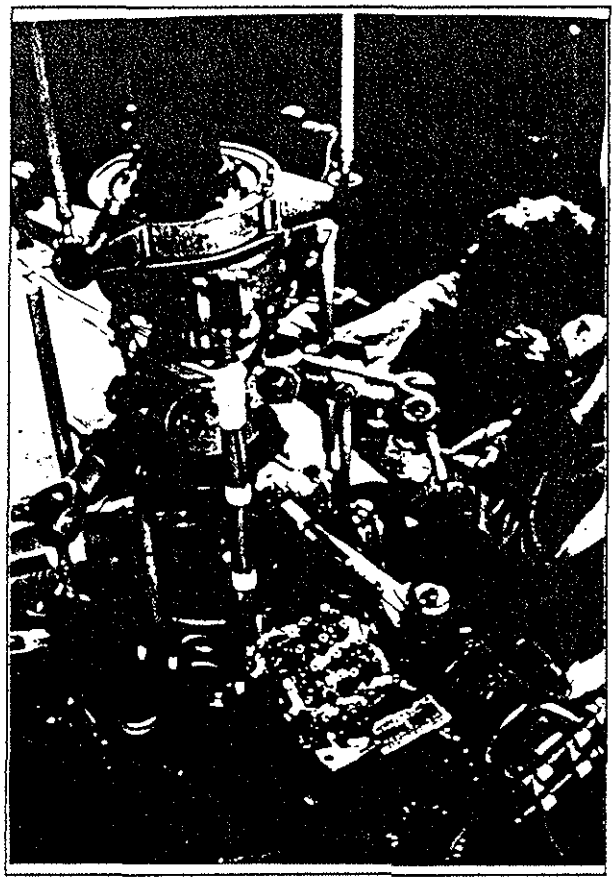

*Fig.5 Telemetric system mounted on the Kamov-26 Helicopter*

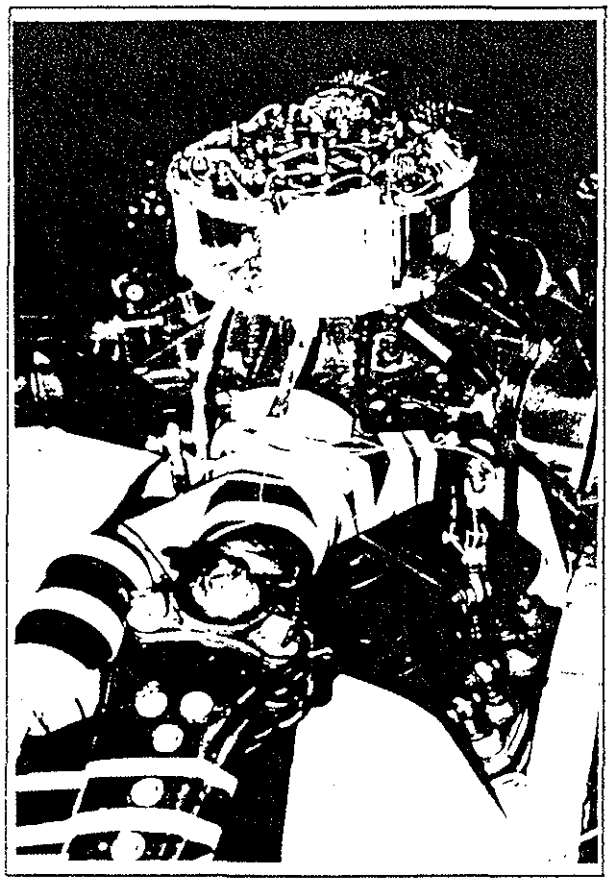

*Fig.6 Telemetric system mounted on the Hughes 500E rotor hub*

The flap angle was measured by a steel strip to which strain gauges were applied. Flapping motion of the blade caused a deformation of the strip resulting in a signal from the gauges. This signal was processed with a calibration factor obtained beforehand in the hangar. The signals were linear in the expected deformation range of the steel strip. This method of measuring the flap angle led to very good results although accuracy lay in the range of $\pm$ 0.25°. This technique was used for flap angle measurement of both helicopters.

The blade position relative to 0° azimuth was measured as well. In case of the Kamov-26 flight tests a micro switch was attached to the rotating part of the lower swash plate. A steel strip fixed to the stationary part of the swash plate activated the switch for a small time intervall during each rotor revolution. The resulting signal allowed a precise positioning of the blade. The Hughes 500E blade position sensor consisted of a light sensitive diode triggered by a steel strip passing through the diode yokes. The diode was attached to the rotating part of the hub and the strip was fixed to a stationary part of the hub assembly. Both methods worked excellent and exact positioning of the blade in the range of $\pm$1° was achieved. The position signals were also used to determine the exact rotor speed during testing.

Flight test data processing

Flight test data recorded on the data tape recorder are analog signals. For evaluation with the RM digitalization of the data is necessary. This was done with a transient recorder (Fig.7). The sampling rate was set such as to have at least five rotor revolutions for each evaluation file. Noise in the data was extracted by filtering the data with a numerical Fourier analysis and synthesis. This was also necessary because the data from the transient recorder had definite stepping in the data values resulting from the numerical processing involved in the digitalization. Filtering and smoothing of the data were performed with practically no signifant alteration of the data information in its time history.

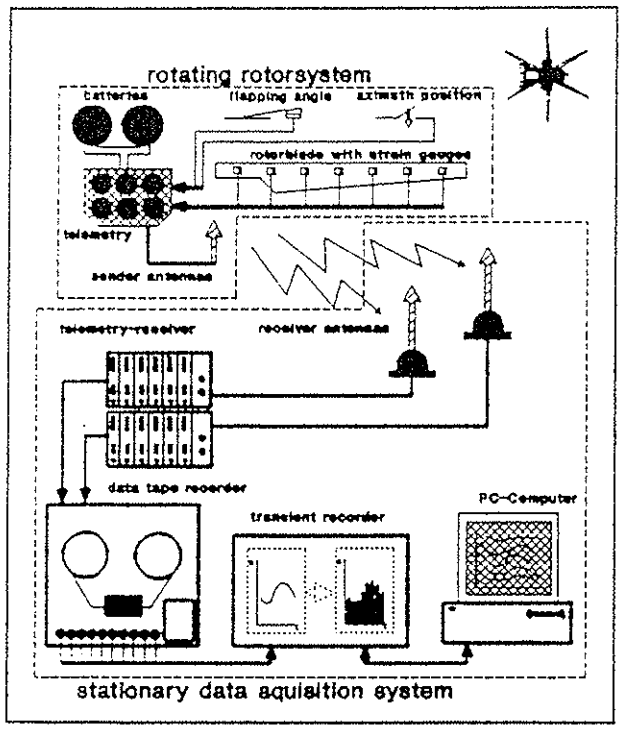


*Fig.7 Data aquisition system for the flight tests with the helicopters*

In Fig.8 an example of the measured strain gauge data for the Kamov-26 at a flight speed of 140 km/h is presented. The depicted moments are the equivalent bending moments resulting from the elastic deformation of the blade. The actual moments are larger for the same transversal loads since the centrifugal influence is not contained in the static calibration factors. The same holds for the measured moments of the Hughes 500E at a flight speed of 100 knots shown in Fig.9.

Comparison shows that the Kamov-26 moments are large in the root area of the blade. The outer part of the the blade is subjected to primarily negative moments meaning a negative deformation i.e. a bending of the blade downward. This is also the case for the Hughes blade. The moments in the blade root area are much smaller meaning a lower stressing of the blade structure. The time histories of both data sets lead to the conclusion, that significant dynamic effects are experienced by the blades. A change from mainly negative moments to positive moments is seen for the retreating part of the blades.

Reconstruction results

The reconstructed forces on the blade are local forces. The rotor blade is modelled as a beam with lumped masses at definite locations (Fig.3). The RM is a discretized numerical method and accordingly the reconstructed forces are located at the mass locations. A smaller spacing between the strain gauges would result in a better reconstruction of the spanwise air load distribution. The same

holds for an adequate spacing of the masses and their locations. Keeping this in mind the following reconstructed forces show very good results in representing the spanwise air load distribution on the blades. Further refinement of the RM is presently undertaken.

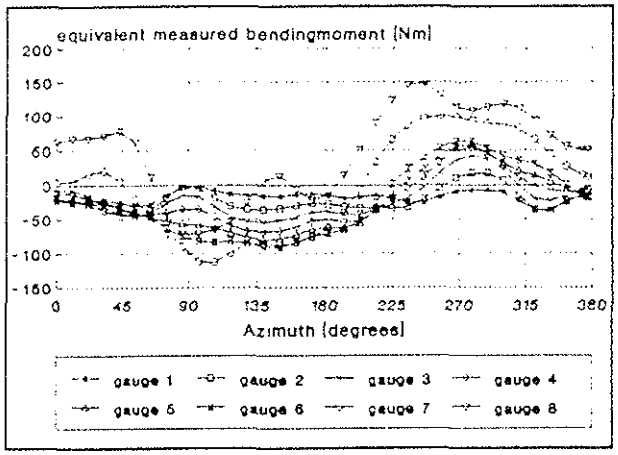


*Fig.8 measured equivalent bending moments of the Kamov-26 at 140 km/h flight speed*

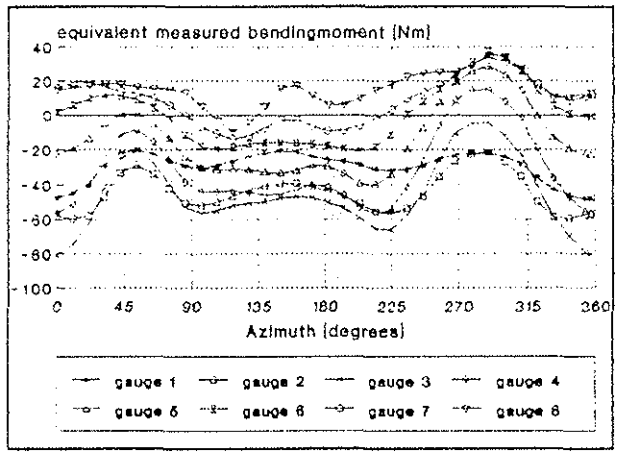


*Fig.9 measured equivalent bending moments of the Hughes 500E at 100 knots flight speed*

As a typical example of a hovering flight reconstruction for one rotor revolution, Fig.10 shows the case of the Hughes 500E hovering in 20 meters altitude. The depicted force distribution is as would be expected and the total lift derived from the reconstructed forces equals the helicopter weight. At the blade tip a disturbance of the distribution is noted which may be caused by a BVI with a tip vortex of the preceding blade. The uniform distribution for all shown azimuth positions is typical for hovering flight. An evaluation of the rolling and pitching moments of the helicopter from the reconstructed forces shows for both a very small value. Reconstruction for flight altitudes of 2 and 10 meters show more or less the same results. A clear distinction of ground effects could not be noted at the present level of evaluation. Refined evaluation of the hovering test data will hopefully result in distincter representation of ground proximity effects.

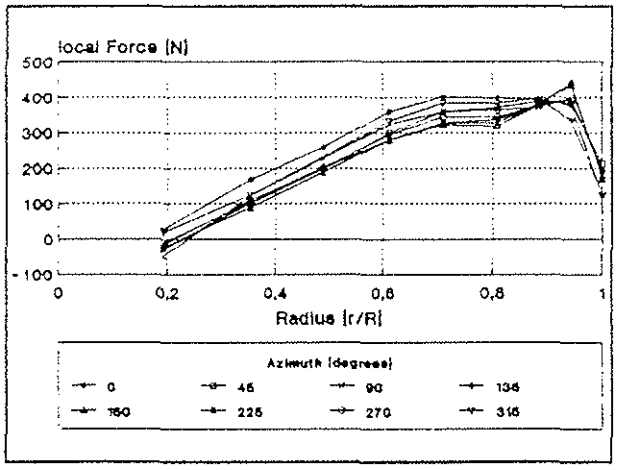


*Fig.10 reconstructed local forces for the hovering Hughes 500E at 20 meters altitude*

From the numerous forward flight reconstructions three will be presented in the following as typical examples of the RM results. These are forward flights of the Kamov-26 at 140 km/h and the Hughes 500E at 100 and 20 knots. The Kamov-26 rotor speed is 275 RPM with a mean collective angle of attack of 8°-9°. The advance ratio is 0,207. The rotor speed for the Hughes 500E is 490 RPM and 9° collective. The advance ratio is here 0,24. Flight altitude was in both cases about 50-60 meters.

In forward flight at 140 km/h the Kamov-26 blade experiences some notable aerodynamic effects as shown in Fig.11. Due to the rotor rotation and the change in cyclic pitch the advancing blade (0°-180°) is more loaded in the inner part than at the tip. The retreating blade on the other hand has a load maximum at the blade tip. In the root area a small negative force can be noted. This is the result of negative air speed at the blade due to the forward flight speed of the helicopter. In Fig.12 a qualitative representation of the reconstructed forces is shown. The line at the lower left part of Fig.12 represents the 0° azimuth position of the blade. The blade rotates counterclockwise. The disturbances at about 220° azimuth may result from BVI but this is not definitely known.

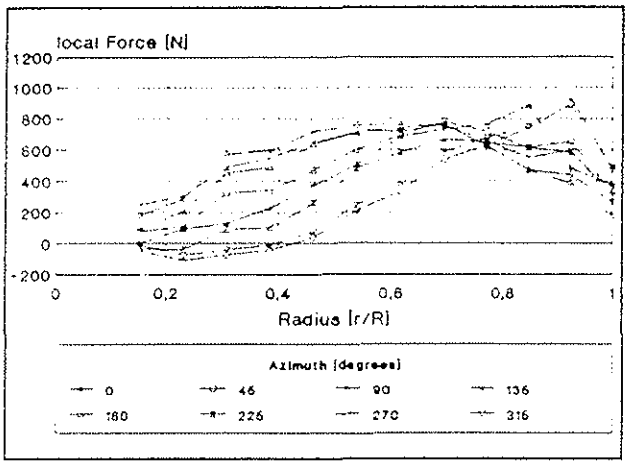


*Fig.11 reconstructed local force of the Kamov-26 at 140 km/h forward flight speed*

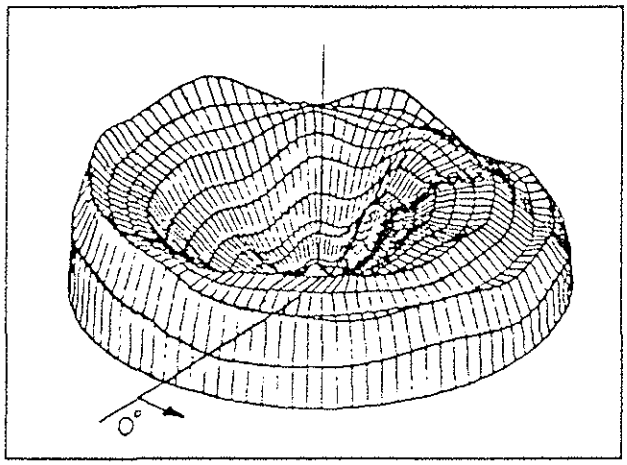


*Fig.12 reconstructed local force of the Kamov-26 at 140 km/h forward flight speed*

The reconstructed force in Fig.13 for the Hughes 500E at 100 knots flight speed shows more or less the same effects as seen with the Kamov-26. The advancing blade experiences a lift maximum in the middle of the blade at about 180°. Compared with the Kamov-26 a more uniform distribution during one rotor revolution is present. In Fig.14 the qualitative representation of the forces show at 0° azimuth a strong disturbance in the distribution. This may result from an interaction of the tail fuselage assembly, tip vortices and the blade. This effect is present for all higher flight speeds of the Hughes 500E helicopter and vanishes for lower speeds. At about 80° and 280° weak BVI may be seen.

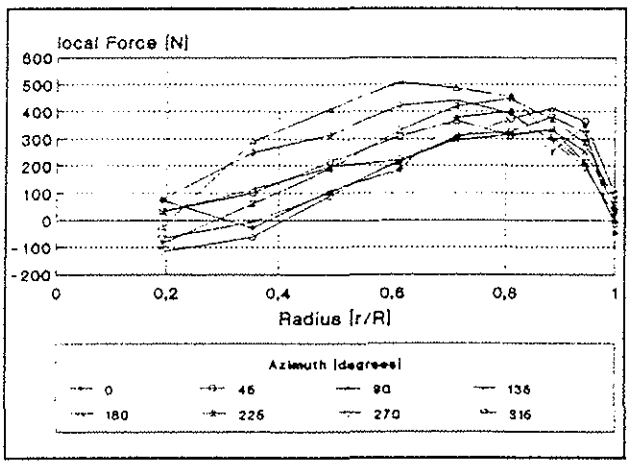


*Fig.13 reconstructed local force of the Hughes 500E at 100 knots forward flight speed*

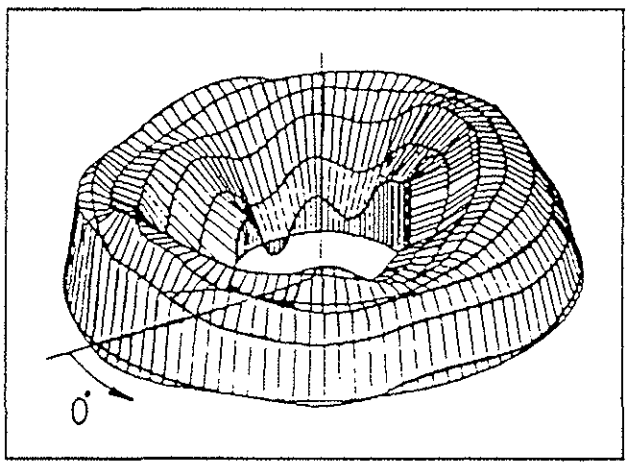


*Fig.14 reconstructed local force of the Hughes 500E at 100 knots forward flight speed*

A very interesting case is the forward flight of the Hughes 500E at 20 knots with an advance ratio of 0.05. Fig.15 shows the reconstructed force for blade azimuth positions of 68° to 117°. At this low flight speed distinct BVI occur. At 68° the blade encounters a tip vortex which shows considerable influence on the spanwise force distribution as the interaction continues. The BVI wanders from the blade tip to the inner part of the blade as the blade rotates further. This typical effect is expected and the reconstruction result shows the BVI very clearly. At this flight speed and due to the relative high number of blades in the rotor more BVI should be present regarding possible interaction locations. In Fig.16 only two distinct BVI belonging actually to the same tip vortex can be seen. The helicopter is in forward flight and the tip vortices from the preceding blades are washed away from the rotor by the air stream and the rotor downwash. It seems as if the tip vortex of the immediately

preceding blade is the only one still close enough to the blade to induce any significant disturbance in the load distribution. The exact location of the tip vortices of the Hughes 500E during BVI is not known and further investigation to clarify this is necessary. Comparison between Fig.14 and 15 shows that the disturbance noted at 0° in Fig.14 is not or only very weakly present in Fig.16.

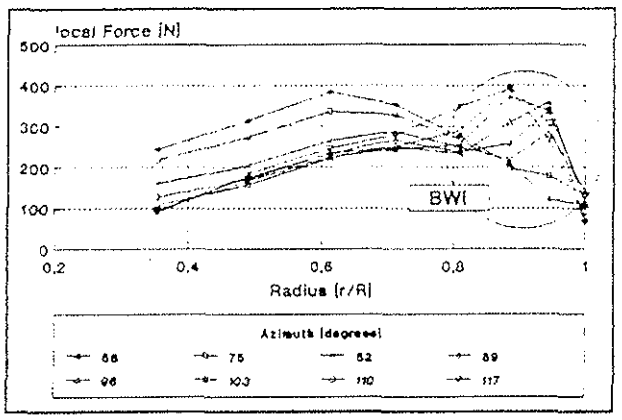


*Fig.15 reconstructed local force of the Hughes 500E at 20 knots forward flight speed*

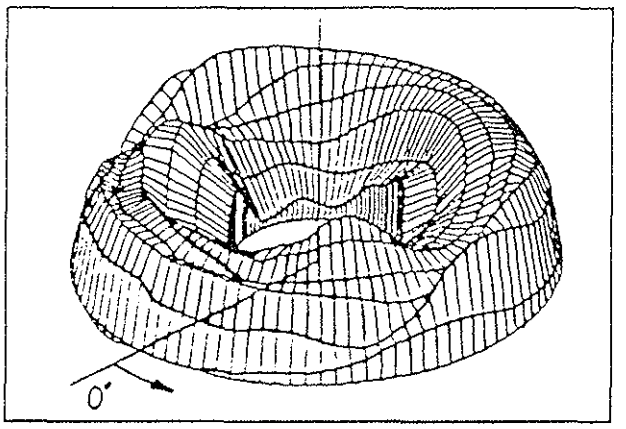


*Fig.16 reconstructed local force of the Hughes 500E at 20 knots forward flight speed*

In Fig.17 the reconstructed forces for mass nr. 2 of the Hughes 500E helicopter at 20 knots flight speed are shown. The total force results from the elastic properties of the blade as if the air load were applied quasistatically. The dynamic force is the mass inertia computed from the blade motion and the mass at this location. The dark line is the reconstructed local force at the mass nr. 2 of the lumped mass model in Fig.3 (see also Eq.(9)). Two distinct BVI are present. As the blade encounters the tip vortex at about 50° the force first decreases and then increases again. Looking at the rotational orientation of the vortex this should be expected. The contrary is seen in the BVI at about 270°. Here first an increase of the reconstructed force followed by a decrease is noted. This too is correct for a BVI at this location. In Fig.18 the reconstructed forces at the masses 1 to 8 (respectivly radiuses r/R) of the Hughes 500E blade are presented in a qualitative manner to show the BVI development during the rotor rotation more clearly. The stippled lines connect the reconstructed BVI at the mass locations. As a comparison Fig.19 shows the BVI locations for a two bladed model rotor tested in the wind tunnel [Ref.4]. The advance ratio is 0,175 and the rotor diameter is 1,1m. Blade chord is 0,055m and the profile a NACA 0012. Rotor speed is 1000 RPM.

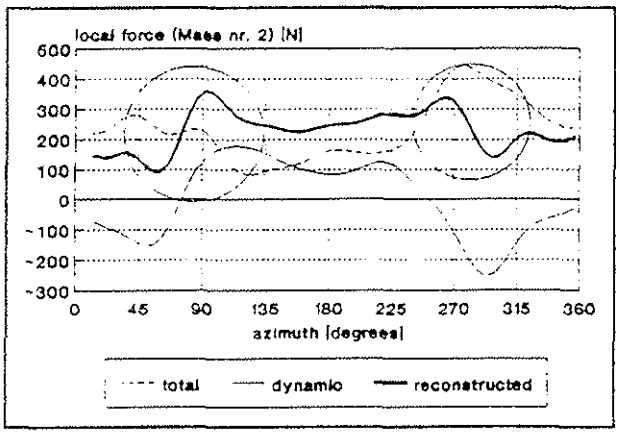


*Fig.17 reconstructed local force at mass nr. 2 for the Hughes 500E at 20 knots forward flight speed*

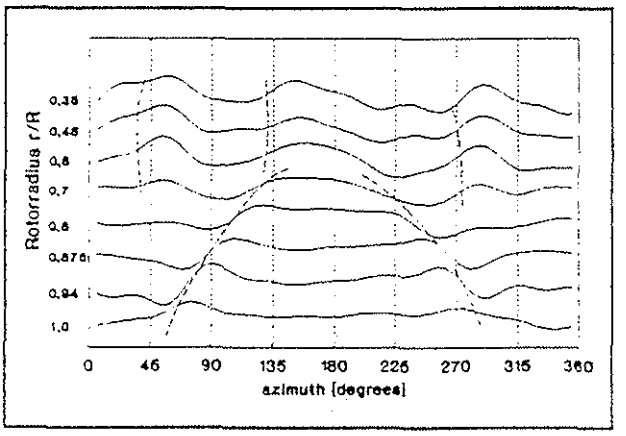


*Fig.18 qual. diagram of the reconstructed force of the Hughes 500E at 20 knots forward flight speed*

## Concluding remarks

The reconstruction of the acting forces on a rotating blade from measured structural response data with the above mentioned reconstruction method (RM) has been proven to be very succesful in the evaluation of wind tunnel and flight test data. Reconstruction of air load distribution on the blade showed very good results for both helicopter types although only eight strain gauge signals per blade were measured. The data aquisition system with the telemetric system as central part worked very well and its further use in helicopter testing recommendable.

Reconstruction of hovering flights show the expected load distributions and the total lifts derived from the reconstructed forces agree very well with the measured helicopter weights. In some evaluations Blade-Vortex-Interactions (BVI) in the blade tip region are present. In forward flight the dynamic effects from blade motion and unsteady aerodynamic loads show very clearly in the reconstruction results. A notable difference for the advancing and retreating blade can be seen. Spanwise distributions are as should be expected and BVI are present at the appropiate locations in the manner described by theory. In case of the Hughes 500E a notable disturbance is present at high flight speeds at the 0° azimuth position which may result from the interaction between the tail fuselage assembly, blade tip vortices and the blade.

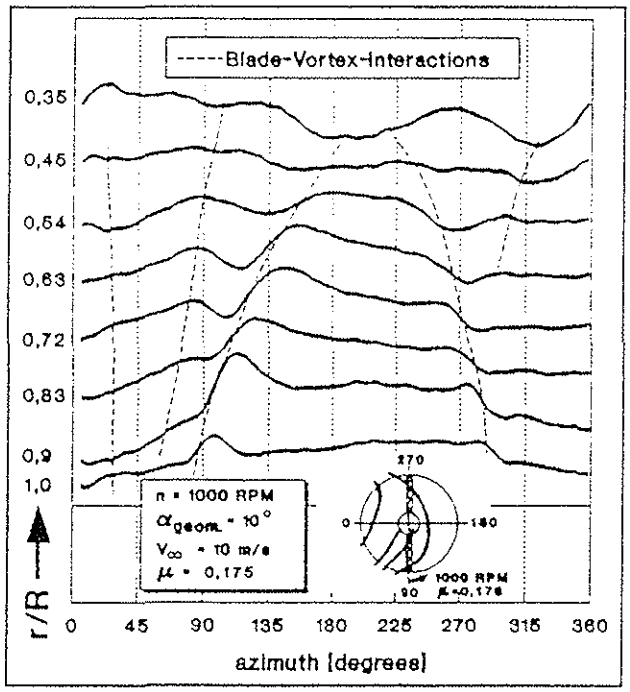


*Fig19. BWI for a two bladed model rotor in wind tunnel test*

From the reconstruction results and their critical evaluation we conclude, that the RM can be used to investigate the aerodynamic effects and forces on the rotating blade of a helicopter in the time and geometric domain. High sampling rates are possible which enable the evaluation of very fast aerodynamic effects as e.g. the BVI reconstructed for the Hughes 500E forward flight at 20 knots speed. A relative low number of structural response measurement devices is required to achieve very good reconstruction results. Furthermore, comparing pressure measurement techniques with the RM, the RM not only gives the blade air load distribution but also e.g. the elastic blade deformation and the forces from inertia. The RM recommends itself as an easy to use and cost effective alternative to complex pressure measurements on rotating blades, aeroplane wings and aerospace structures or, in fact, for determining the acting forces on any technical or architectural structure.

## Acknowledgements

This paper presents results of research work conducted in Project C3 of the Sonderforschungsbereich 25 sponsored by the Deutsche Forschungsgemeinschaft (DFG). The flight tests were possible only with considerable help from the Hungarian Air Service which provided the Kamov-26 and Hughes 500E helicopters for testing and allowed the use of the facillities at Budaörs airport. We would also like to thank our hungarian partners of the aeronautical department at the Technical University in Budapest, Dr. Istvan Steiger and Dr. Tamas Gausz as well as Dr. Istvan Gyurkovics of the Hungarian Air Service for their considerable help during the flight testing in Hungary.

## References

1. J. Scheiman; L.H. Ludi: Qualitative evaluation of effect of helicopter rotor blade tip vortex on blade airloads. NASA-TN-D-1637, 1963

2. H. Öry; H. Glaser; D. Holzdeppe: Transient external loads or interface forces reconstructed from structural response measurements. International Conference Spacecraft Structures. 12/1985 Toulouse, France.

3. D. Holzdeppe: Beitrag zur versuchstechnischen Ermittlung der instationären aerodynamischen Belastungen eines Rotorblattes aus Messungen mechanischer Reaktionen des elastischen Systems. Dissertation an der RWTH-Aachen 1987

4. H. Öry; H.W. Lindert: Ermittlung der Luftkraftverteilung am rotierenden Rotorblatt aus gemessenen Strukturreaktionen. To be presented at the DGLR-Jahrestagung September 1992 and published in the proceeding papers.

5. A.R. Walker; D.P.Payen: Experimental application of strain gauge pattern analysis (SPA)-Windtunnel and flight test results. Royal Aerospace Establishment, Farnborough, England. Vertica Vol.14 , No. 3 pp. 345-359, 1990

6. D. Williams: The principals underlying the dynamic stressing of aeroplanes. Journal of the Royal Aeronautical Society, 1951 pp.362-381.

7. H.W. Lindert; H. Öry: Arbeits- und Ergebnisberichte des Teilprojektes C3 des Sonderforschungsbereiches 25 der Deutschen Forschungs Gesellschaft (DFG)

8. R.R.Craig Jr.: Structural Dynamics - An Introduction to Computer Methods. John Wiley & Sons 1981